Proceedings of the
International Conference on Mechanical Engineering and Renewable Energy 2015
(ICMERE2015) 26 – 29 November, 2015, Chittagong, Bangladesh

ICMERE2015-PI-233

EXPERIMENTAL STUDY OF PASSIVE FLOW SEPARATION CONTROL OVER A NACA 0012 AIRFOIL

Mahbubur Rahman[1,*], Md. Amzad Hossain[2], Md. Nizam Uddin[3] and Mohammad Mashud[4]

[1-4]Department of Mechanical Engineering, Khulna University of Engineering & Technology, Khulna-9203, Bangladesh
[1,*]Mahbubmithu75@gmail.com, [2]amzad59@gmail.com,[3]engrnizam02@gmail.com, [4]mdmashud@yahoo.com

Abstract*- This paper is focused on experimental investigation of subsonic flow separation over a NACA0012 airfoil with 00 to 200 angle of attack and flow separation control with vortex generators. The addition of vortex generator (VG) results in increased lift-coefficient and reduced drag-coefficient at large incident angles. The influence of VG on the fluid flow and aerodynamic forces acting on the airfoil are reported in this paper. The ability to manipulate a flow passively or actively is of immense technological importance. This paper is more concentrating on modern passive flow control by using vortex generator methods. These methods are used majorly to achieve drag reduction, lift enhancement, flow separation control etc. The test conducted in subsonic wind tunnel of 1m×1m rectangular test section at flow speed 25m/s placing the airfoil without vortex generator and with vortex generator inclination at angle of attack ranging from 0 to 20 degree. The test result shows a considerable amount of reduction in drag coefficient and increase in lift coefficient by using vortex generator. Comparison of pressure coefficient, lift coefficient, drag coefficient between the airfoil without the vortex generator and with vortex generator fitted airfoil help us to understand how the vortex generator energies the boundary layer flow and hence delay the stall*

Keywords: Flow separation, Vortex generator, Passive flow control

1. INTRODUCTION

At low angle of attack (α), the flow over an airfoil is smooth and attached. When α is increased, the co-efficient of lift is increased as the pressure difference between the suction and pressure surface of the airfoil is enhanced. However, after a particular α, known as stalling angle, the flow will not able to withstand the adverse pressure gradient generated over the suction side of the foil and as a result the boundary layer separation will take place. This phenomenon is known as stalling which results in loss of lift, increased drag, and generation of aerodynamic noise. An aircraft is required to operate at high α during takeoff, landing and maneuvering. Hence flow control over an airfoil at high angle of attack is of strong interest [1]. At low Reynolds number, the boundary layer on the upper surface of an airfoil at incidence remains laminar at the onset of pressure recovery. As laminar flow is less resistant to an adverse pressure gradient, flow separation may occur near the leading edge of the airfoil. The separated shear layer is in viscidly unstable and vortices are formed [2]. The detached shear layer may also undergo rapid transition to turbulence and the separated flow may reattach to the wall surface because of the increased entrainment associated with the turbulent flow [3] and form an attached turbulent boundary layer. Many passive flow control devices are employed to mitigate the aforementioned adverse effects by delaying or suppressing the separation, and thereby widen the α range of aircraft wing (Gad-el-Hak, 1991).

The concept of VG is first introduced by Taylor, 1947. He has shown that the stream wise trailing vortices generated over a row of small plates increased the stream wise momentum and hence delay the flow separation in a diffuser. The conventional passive vortex generator was first developed by Taylor [4] in 1947 to prevent boundary-layer separation in wind tunnel diffuser. The first systematic study of vortex generations and their effects on the boundary-layer was performed by Schubauer and Spangenberg [5] in late 1950's.Since then the vortex generators have been successfully applied to lifting surfaces in many aeronautical applications for control of flow separation and reduction of drag in a turbulent boundary layer [7, 8, 9]. The vortices created by vortex generators transfer low energy fluid from the surface into the mainstream, and bring higher energy fluid from the mainstream down to the surface where the higher kinetic energy level is able to withstand a greater pressure rise before separation occurs. Another mechanism introduced by the vortex generator is associated with the excitation of the local instability waves that lead to an early transition to turbulence, which delays the flow separation and reduces the size of the separation zone. Subsequently many tests have been

performed to show the effectiveness of VGs as a flow control device [1].

Generally, vortex generators are designed as either passive or active devices. The effectiveness of a passive vortex generator, whose size, position, and orientation are fixed on the surface, is limited to a narrow operational range. Lin [10] gave an in-depth review of boundary layer flow separation control by the passive low-profile vortex generators.

Vortex generators (VGs) are an array of small vanes attached perpendicularly over the suction surface of the wings and in turbo machine blades. These vanes are fixed at a small incident angle relative airflow. VGs enhance the ability of the fluid to stick with the wing surface even at large α by increasing the momentum transfer from the free-stream flow into the boundary layer [1]. Flow control through boundary layer manipulation to prevent or postpone separation can significantly reduce the pressure drag, enhance the lift, and improve the performance of the aircraft. Traditionally, flow separation control is implemented through airfoil shaping, surface cooling, moving walls, tripping early transition to turbulence, and near-wall momentum addition [2].The aim of this paper is to control the passive flow separation of a NACA 0012 airfoil by using vortex generator.

2. AIRFOIL DESIGN & DESCRIPTION

The airfoil sections of all NACA families considered herein are obtained by combining a mean line and a thickness distribution. The necessary geometric data and some theoretical aerodynamic data for the mean lines and thickness distributions obtained from the supplementary figures by the methods described for each family of airfoils. The process for combining a mean line and a thickness distribution to obtain the desired cambered airfoil section is shown in figure below.

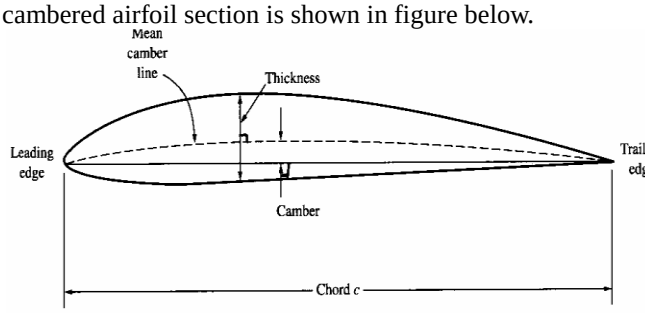

Fig. 1: A typical airfoil

The cross sectional shape obtained by the intersection of the wing with the perpendicular plane is called an airfoil. The major design feature of an airfoil is the mean cambered line, which is the locus of points halfway between the upper and lower surfaces as measured perpendicular to the mean cambered line itself. The most forward and rearward points of the mean cambered line are the leading and trailing edges respectively. The straight line connecting the leading and trailing edges is the chord line of the airfoil and the precise distance from the leading to the trailing edge measured along the chord line is simply designated the chord of the airfoil, given by the symbol C. The camber is the maximum distance between the mean camber line and the chord line, measured perpendicular to the chord line. The camber, the shape of the mean camber line and to a lesser extent, the thickness distribution of the airfoil essentially controls the lift and moment characteristics of the airfoil. For symmetrical airfoil the mean camber line coincide with chord line.

If X_u and Y_u represent respectively the abscissa and ordinate of a typical point of the upper surface of a symmetrical airfoil and y_t is the ordinate of the symmetrical thickness distribution at chord wise position X_1, the upper surface coordinates are given by the flowing relations

X_u= x

Y_u= y_t

The corresponding expressions for the lower surface co-ordinates are

X_l = x

Y_l = -y_t

3. AIRFOIL DESCRIPTION OF NACA 0012

For NACA 0012

Chord of airfoil, c = 1

For symmetric airfoil mean chamber line coincide with chord line so for NACA 0012 there is no chamber

Maximum wing thickness, t = last two digit × %c

=12 × 1/100

=0.12

By applying C++ Programming Language the surface profile of the airfoil was generated by using basic equation of airfoil

The formula for the shape of a NACA 00xx foil, with "xx" being replaced by the percentage of thickness to chord, is:

$$y_t = \frac{t}{0.2}c\left[0.2969\sqrt{\frac{x}{c}} - 0.1260\left(\frac{x}{c}\right) - 0.3516\left(\frac{x}{c}\right)^2 + 0.2843\left(\frac{x}{c}\right)^3 - 0.1015\left(\frac{x}{c}\right)^4\right],$$

Where,

c= is the chord length,

x =is the position along the chord from 0 to c,

y =is the half thickness at a given value of x (centerline to surface), and

t= is the maximum thickness as a fraction of the chord (so 100 t gives the last two digits in the NACA 4-digit denomination).

In this equation, at (x/c) = 1 (the trailing edge of the airfoil), the thickness is not quite zero. If a zero-thickness trailing edge is required, for example for computational work, one of the coefficients should be modified such that they sum to zero. Modifying the last coefficient (i.e. to -0.1036) will result in the smallest change to the overall shape of the airfoil. The leading edge approximates a cylinder with a radius of:

$$r = 1.1019\,t^2.$$

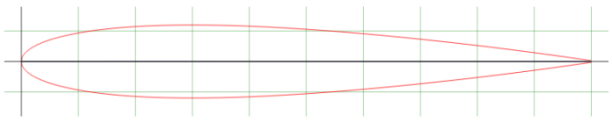

Fig.2 Profile of NACA 0012 airfoil

4. MODEL CONSTRUCTION

By applying Computer C Programming Language the regular surface profile of the NACA 0012 model was made. The chord length of the model is 35 cm an with span of 35cm. Thus the chord length based Reynolds number relevant at low flight speeds, which are a concern for the exploration of wing formation mechanism, is estimate to be about 105. The chord length of the model was determined to have Reynolds number of the same order. The airfoil used to construct the whole structure is NACA 0012. After the model has been constructed then it is time to construct the vortex generator. Fig. 2.3.1(a) shows the layout of a pair of vortex generators on the surface of the airfoil, similar to the experiment of [13] except that the flat plate used in the experiment is replaced by the NACA0012 airfoil. The width of the airfoil is set to 0.1Cin. The circular wing lip type vortex generator has a radius of 0.01675Cand a thickness of 0.001C. The vortex generator can rotate about its circular center (apex of the vortex generator) with a pitch angle ranging from 0°to 30.96°as shown in Fig. 3. The 0°pitch angle is corresponding to the fully retracted position and 30.96°to the fully deployed position. The maximum pitch of the vortex generator gives it a maximum height of 0.0086Cnormal to the airfoil surface. On the surface of the airfoil, the apex of the vortex generator is located at x= 0.1C, as shown in Fig. 3(c). The distance between the mid-chord points of the vortex generators is 0.02C. The angle of yaw to the free stream flow is 18°. In the passive flow control, the vortex generators were deployed to their maximum height.

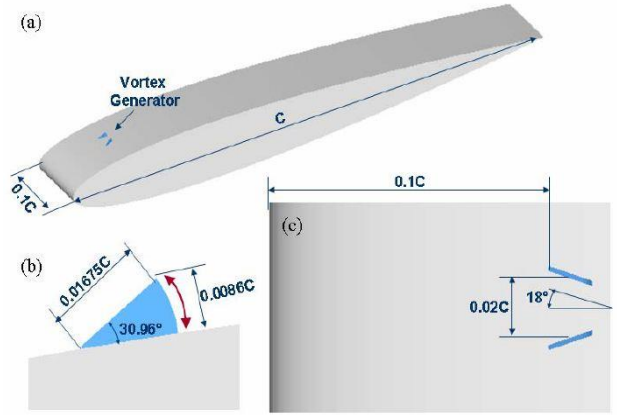

Fig.3: Design of NACA0012 airfoil and vortex generator (a) perspective view; (b) side view; (c) top view

Fig 4: Constructed airfoil of NACA 0012

Fig.5: Constructed airfoil with vortex generator

5. EXPERIMENTAL SETUP

Experiments were conducted in the Aerodynamics Laboratory Department of Mechanical Engineering (Khulna University of Engineering & Technology) with subsonic wind tunnel of 1 m× 1 m rectangular test section. The wind tunnel could be operated at a maximum air speed of 43 m/s and the turntable had a capacity for setting an angle of attack of 45 degree. A small sized model is appropriate to examine the aerodynamic characteristics for the experiments. If we desire to examine the aerodynamic characteristics of a large model, a large scale wind tunnel facility is necessary for test. Furthermore, it would be difficult to support the airfoil with a desirable attitude in these wind tunnel experiments. Since the vertical part of the aerodynamic force produces the lifting force necessary to suspend the load. The model was placed in the testing section of the wind tunnel. Then the testing procedure is started of measuring the pressure of the constructed model at different point from leading edge to trailing edge along chord line from the pressure sensor reading. Figure (5) shows a photograph of the airfoil with vortex generator, which is mounted horizontally in the test section of the wind tunnel.

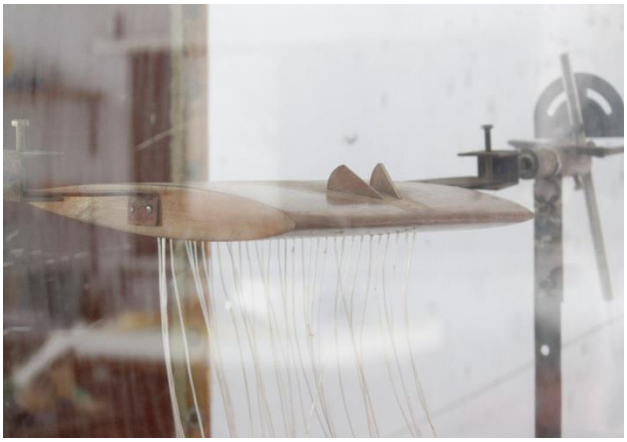

Fig.6: Experimental setup of airfoil with vortex generator.

6. EXPERIMENTAL PROCEDURE

For the complete testing the constructed model, subsonic wind tunnel and pressure measuring instrument were used as required apparatus. At the first step of the experimental procedure the constructed model aircraft with NACA 0012 without vortex generator was placed inside the testing section of the wind tunnel. By placing airfoil without vortex generator the testing section was closed to start the measurement. For different angle of attack ranging from (0^0 to 20^0)pressure on the upper and lower surfaces were measured. After this the airfoil with vortex generator was placed in the wind tunnel and pressures on the upper and lower surfaces were measured. For different angle of attack ranging from(0^0 to 20^0)pressure on the upper and lower surfaces were measured. The velocity of the wind tunnel was controlled by a regulator attached with the wind tunnel. The ambient pressure, temperature and humidity were recorded using barometer, thermometer, and hygrometer respectively for the evaluation of air density in the laboratory environment. The tests were carried out with free-stream velocity of 25m/s. When the measurement of data had been complete then the calculation process was started. From the measured pressure the lift coefficient and drag coefficient was calculated by using the mathematical relation.

Lift and drag coefficient can be defined as follow

$$C_L = \frac{1}{c}\int_0^c (C_{pl} - C_{pu})\,dx$$

$$C_D = \frac{1}{c}\int_0^c \left(C_{pl}\frac{dy}{dx} - C_{pu}\frac{dy}{dx}\right)dx$$

Where,

C_{pl} = pressure coefficient at lower surface

C_{pu} = Pressure coefficient at upper surface

Pressure coefficient is defined as,

$$C_p = \frac{P - P_\infty}{\frac{1}{2}\rho_\infty v_\infty^2}$$

Where,

P = local pressure

P_∞ = free stream pressure

v_∞ = Free stream velocity

ρ_∞ = Free stream density

$$Re = \frac{\rho_\infty v_\infty c}{\mu_\infty}$$

7. RESULTS & DISCUSSION

7.1 Effect of VG on Cp distribution

With the airfoil with and without vortex generator the wind tunnel measurements were done. The pressure coefficient, coefficient of lift and the coefficient of drag have been calculated from the experimental results. Also various graphs have been drawn to examine the measured and calculated data nature. Figure 4.1.1 to 4.1.4 shows the distribution of pressure coefficient (Cp) over the airfoil at different angles of attack without and with vortex generator. The experimental results show that the addition of VGs has only minor influence in the Cp distribution. Except near the VG locations, the Cp of with and without VG coincide. In the clean airfoil, the Cp achieves a minimum value near the leading-edge, owing to acceleration of the fluid flow over the top surface of the foil. Just after the peak value, the Cp increases along the downstream creating a strong adverse pressure gradient. This causes the boundary layer to separate from the top surface. Though, with the addition of VGs, the maximum suction peak remains the same, the subsequent rate of increase of Cp is less when compared to that of clean airfoil case. This is advantageous in two ways. Firstly, the adverse pressure gradient over the airfoil is decreased and hence the stalling is avoided. Secondly, the suction pressure prevails over most of the top surface of the foil. This results as increase in CL at the same operating α.

7.2 Effect of VG on Aerodynamic forces

The lift coefficient characteristics of the airfoil model under test are shown in Figure 4.2.1. The lift increases with increase in angle of attack to a maximum value and thereby decreases with further increase in angle of attack. The initial value of lift coefficient at zero angle of attack for a chord based Reynolds number 1.58 × 105 is 0.031 instead of 0 because of inaccuracy during constructing the wing. The variation of lift (CL) and drag coefficient (CD) with respect to the angle of attack are shown in figure 4.2.1 and 4.2.2.At low α the difference between the clean airfoil and that fitted with VG is not significant. However, for a clean airfoil, the CL decreases rapidly and CD increases gradually as seen from figure 4.2.1 and 4.2.2 and CD shows a sharp increase at α=14 degree.From this, it can be inferred that the clean airfoil is stalled at this α.In contrary to this , the airfoil with VGs does not show any sign of stalling until α=16 degree, since throughout the range of α considered, the CL as well as CD increases gradually as can be seen from the figure. This result demonstrates the stall-delaying effect of vortex generators at high angle of attack flow over the airfoil. The CD of attached VG airfoil is higher than that of clean airfoil at low α(Fig 4.2.2),because at such low α the skin friction drag produced over the foil dominates the pressure drag due to the streamlined shape of the foil. Since the addition of VGs increases the wetting surface area available for the flow, the increase in CD is observed. Moreover, the tip vortex produced from the VG also adds up to additional drag. As α is increased the contribution of pressure drag to the total drag is increased

since the separation takes place at large α.The separation is delayed in airfoil with attached VG. Hence CD of attached VG case is lower than that of clean airfoil.

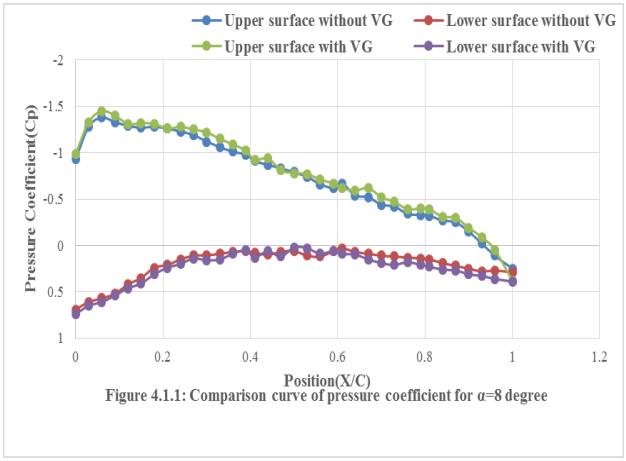

Figure 4.1.1: Comparison curve of pressure coefficient for α=8 degree

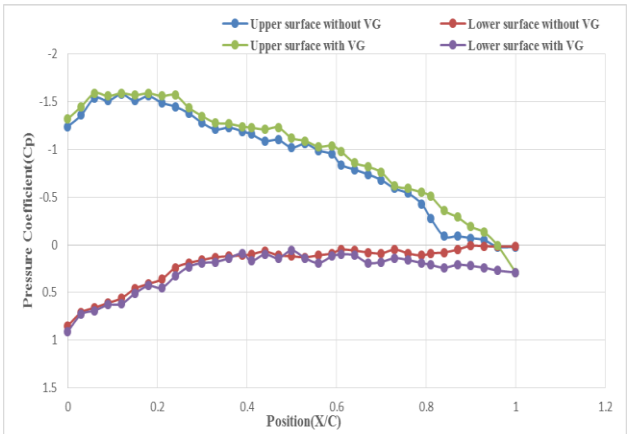

Figure 4.1.2: Comparison curve of pressure coefficient for α=14 degree

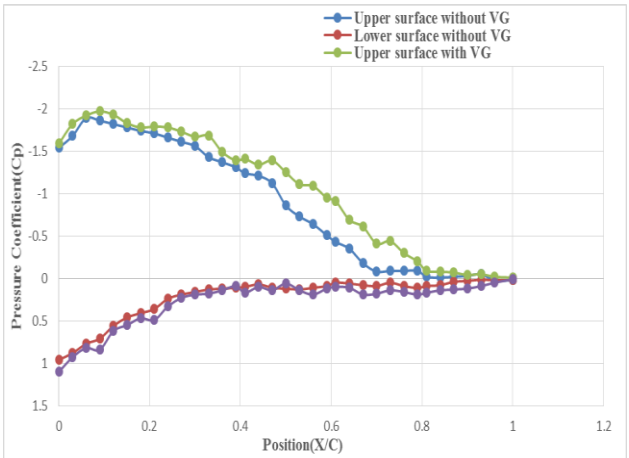

Figure 4.1.3: Comparison curve of pressure coefficient for α=18 degree

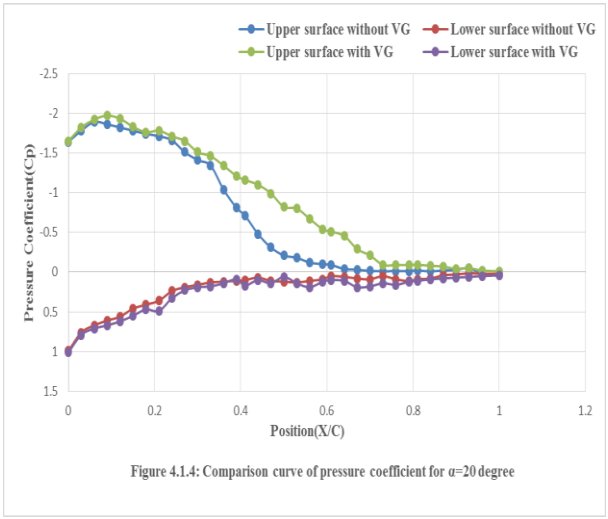

Figure 4.1.4: Comparison curve of pressure coefficient for α=20 degree

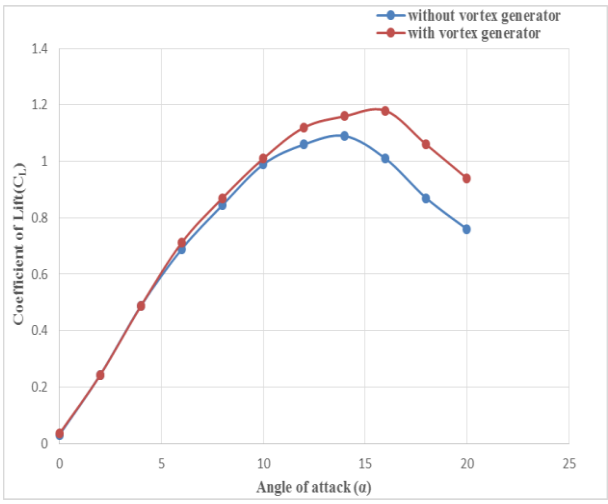

Fig.6: Comparison of CL vs α with and without vortex generator

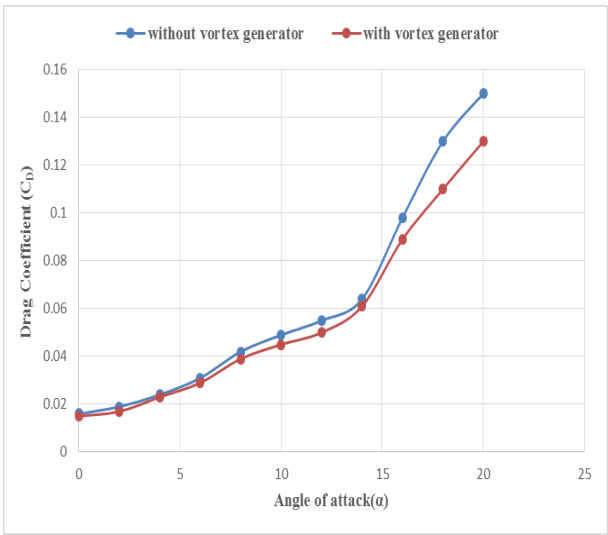

Fig 7: Comparison of CD vs α with and without vortex generator

8. ACKOWLEDGEMENT

My sincere acknowledgments to Dr. Mohammad Mashud, Professor of the Department of Mechanical Engineering of Khulna University of Engineering & Technology (KUET) for his support and guidance.

9. REFERENCES

[1] U. Anand, Y. Sudhakar, R. Thileepanragu, V.T. Gopinathan, R. Rajasekar, "Passive flow control over NACA 0012 aerofoil using vortex generators" proceeding of the 37th National and 4th International Conference on Fluid Mechanics and Fluid Power.December 16-18,2010,IIT Madras,Chennai,India.

[2] Alam, M. and Sandham, N.D. 2000 Direct numerical simulation of 'short' laminar separation bubbles with turbulent reattachment. J. Fluid Mech.410, 1-28.

[3] Gad-el_Hak, M. 2000 Flow Control, Passive, Active, and Reactive Flow Management, Cambridge University Press.

[4] Taylor, H.D. 1947 the elimination of diffuser separation by vortex generators. United Aircraft Corporation Report No. R-4012-3.

[5] Schubauer, G.B., Spangenberg, W.G. 1960 Forced mixing in boundary layers. J. Fluid Mech.8, 10-32.

[6] Casper, J., Lin, J.C., Yao, C.S. 2003 Effectof sub-boundary layer vortex generators on incident turbulence. AIAA Paper2003-4162.

[7] Hutchines, N., Choi, K-S. 2001 Experimentalinvestigation of turbulence suppression by the imposition of a large-scale vortical control flow. AIAA Paper 2001-2775

[8] Kerho, M., Kramer, B. 2003 Enhanced airfoil design incorporating boundary layer mixing devices. AIAA Paper2003-0211.

[9] Lin, J.C. 2002 Review of research on low-profile vortex generators to control boundary-layer separation. Progress in Aerospace Sciences38, 389–420.

[10] Godard, G., Stanislas, M. 2006 Control of a decelerating boundary layer. Part 1: Optimization of passive vortex generators. Aerospace Science and Technology 10, 181–191.

[11] Shizawa, T., Mizusaki, Y. Response of time-depended flowfield structure behind an active vortex generators pair. AIAA Paper2004-427.

[12] Shizawa, T., Mizusaki, Y. Response of phase-averaged flowfield oflongitudinal vortices to the height of active vortex generators pair. AIAA Paper2005-4885.

[13] Patel, M.P., Carver, R., Lisy, F.J., Prince, T.S., and Ng, T. 2002 Detection and control of flow separation using pressure sensors and miro-vortex generators. AIAA Paper2002-0268.

[14] Osborn, R.F., Kota, S., Geister, D., Lee, M., Tilmann, C. 2001 Active flow control using high frequency compliant structures. AIAA Paper2001-4144.

10. NOMENCLATURE

Symbol	Meaning	Unit
L	Lift force	N
D	Drag force	N
C_l	Coefficient of lift	Dimensionless
C_d	Coefficient of drag	Dimensionless
v_∞	Free stream velocity	m/s
ρ_∞	Free stream density	kg/m^3
μ_∞	Free stream viscosity	m/s
α	Angle of attack	degree
T	Maximum thickness	m
C	Chord length	m
AOA	Angle of attack	degree